

A modified whale optimization algorithm-based adaptive fuzzy logic PID controller for load frequency control of autonomous power generation systems

Raghuraman Sivalingam, Subramani Chinnamuthu & Subhransu Sekhar Dash

To cite this article: Raghuraman Sivalingam, Subramani Chinnamuthu & Subhransu Sekhar Dash (2017) A modified whale optimization algorithm-based adaptive fuzzy logic PID controller for load frequency control of autonomous power generation systems, *Automatika*, 58:4, 410-421, DOI: [10.1080/00051144.2018.1465688](https://doi.org/10.1080/00051144.2018.1465688)

To link to this article: <https://doi.org/10.1080/00051144.2018.1465688>



© 2018 The Author(s). Published by Informa UK Limited, trading as Taylor & Francis Group.



Published online: 22 May 2018.



Submit your article to this journal [↗](#)



Article views: 136



View Crossmark data [↗](#)



A modified whale optimization algorithm-based adaptive fuzzy logic PID controller for load frequency control of autonomous power generation systems

Raghuraman Sivalingam^a, Subramani Chinnamuthu^{ib} and Subhransu Sekhar Dash^{ib}

^aDepartment of Electrical and Electronics Engineering, Velammal Engineering College, Chennai, India; ^bDepartment of Electrical and Electronics Engineering, SRM University, Chennai, India

ABSTRACT

An autonomous power generation system (APGS) contains units such as diesel energy generator, solar photovoltaic units, wind turbine generator and fuel cells along with energy-storing units such as the flywheel energy storage system and battery energy storage system. The components either run at lower/higher power output or may turn on/off at different instants of their operation. Due to this, the conventional controllers will not provide desired performance under varied load conditions. This paper proposes an adaptive fuzzy logic PID (AFPID) controller for load frequency control. In order to achieve an improved performance, a modified whale optimization algorithm (mWOA) was also proposed in this paper for tuning of the AFPID parameters. The proposed algorithm was first evaluated using standard test functions and compared with other recent algorithms to authenticate the competence of algorithm. The proposed mWOA algorithm outperforms PSO, GSA, DE and FEP algorithms in five out of seven unimodal test functions and four out of six multimodal test functions. The effectiveness of the AFPID compared with the conventional PID and the proposed AFPID provides better performance. Reduction of 39.13% in error criteria (objective function) compared with WOA-PID controller. The proposed approach was also compared with some recently proposed frequency control approaches in a widely used two-area test system.

ARTICLE HISTORY

Received 22 December 2017
Accepted 11 April 2018

KEYWORDS

Autonomous power generation system; load frequency control (LFC); whale optimization algorithm (WOA); adaptive fuzzy logic PID controller (AFPID)

1. Introduction

The increasing power demand, rising costs of electricity transmission and distribution, deregulation of the energy markets, depletion of fossil fuels are making a significant entrance of renewable energy resources into the energy sector [1–4]. The centralized power generation, transmission and distribution are now shifting to a decentralized one [1]. In this framework, a new power system model called autonomous power generating system (APGS) has evolved. It is a collection of distributed energy resources (DERs) such as diesel energy generator (DEG), fuel cell (FC), micro-turbine generator (MTG) with solar photovoltaic (PV) units and wind turbine generators (WTG) and cluster of loads [1,2]. The chaotic characteristics of the load and the sustainable energy generations, i.e. wind and solar sources, introduce fluctuations in the system frequency [1]. Energy-storing elements such as ultra capacitor (UC), flywheel energy storage system (FESS) and battery energy storage system (BESS) are coupled to the system to mitigate the unbalance due to generation and load mismatch. These energy-storing devices store the surplus power for a small interval of period from the renewable energy sources and later deliver the

power to the grid when there is a more load demand [5,6]. A proper control strategy is required for coordinating these actions accurately [5]. This calls for the concept of load frequency control (LFC) for damping the frequency oscillation.

To enhance the LFC performance, several approaches such as the conventional PID controller [4,7], robust H_∞ controller [8–11], fractional order controller [1,5,6] have been used in similar types of system design. To preserve desirable performance and stability, either centralized controller [6] or decentralized controller [4, 12] is used. The system parameters and the local loads of the hybrid power system controlled by a centralized control unit rather than multiple decentralized controllers make the overall system design simple as well as reduce cost [1]. Conventional PI-based controller has been adopted by the researcher for LFC on similar types of system [4,7]. Robust H_∞ controller approaches have been widely proposed in the literature for LFC problem [3,9–11]. Few papers addressed fuzzy logic techniques for optimal tuning of the standard PID controller [13–15] and FOPID controller [5] for solving LFC problem. It is observed that adaptive control makes the system under control less affected by the unmodelled

process dynamics and variation in system parameters. Therefore, in the proposed control strategy, an adaptive fuzzy-based PID controller is taken into consideration for LFC in the proposed hybrid power system.

Controlling APGS with various uncertain system parameters is mostly based on optimization [6]. Different types of hybrid algorithms were developed in many papers [1,5,7,8,11,13] to find the controller gains in order to enhance the system transient response as well as to ensure the robustness and stability of the system. Many researchers have suggested different optimization techniques such as fast evolutionary algorithm [16], Glowworm Swarm Optimization [17], multi-objective evolutionary algorithm [18], microgenetic algorithm [19], hybrid differential evolution and harmony search algorithm [20], clustered adaptive teaching learning-based optimization [21] in power system problems. Whale optimization algorithm (WOA) is a recently proposed technique inspired by hunting the behaviour of whales [22]. The major benefit of the WOA technique compared to other established techniques is that the WOA technique does not need specific algorithm parameters. Apart from this, WOA is easy to understand and program. The algorithm uses three operators: the hunt for prey, surrounding the prey and bubble-net searching behaviour of whales for optimization. The superiority of WOA over PSO, GSA, DE and FEP has been demonstrated [22]. However, in original WOA algorithm, the present best solution is the target prey and the others attempt to modify their positions towards the best agent. This process of update may result in being stuck in local optima. Therefore, in the present paper, a modified whale optimization algorithm (mWOA) is proposed where correction factors are introduced at various stages of the algorithm to get improved results. After this, the mWOA technique is used to tune AFPID (adaptive fuzzy logic PID) controller parameters; results are compared with WOA and mWOA optimized PID controller. Deviation in grid frequency, control signal and the output of different controlled sources of APGS system are analysed with standard PID and AFPID controllers and the superiority of the AFPID over PID is demonstrated.

2. Whale optimization algorithm

WOA is a recently proposed meta-heuristic algorithm based on social behaviour of whales [8]. Humpback whales are among the biggest whales whose favourite prey are krill and small fish herds. The hunting process of humpback whales is based on the bubble-net feeding approach method. The twisting bubble-net nourishing scheme is mathematically modelled in WOA. Here the scientific model of encircling prey, spiral bubble-net encouraging move and scan for prey is mathematically expressed.

2.1. Encircling prey

Humpback whale encircles the prey (small fishes); at that point, overhauls its position towards the optimum solution over the course of increasing number of iterations from start to a maximum number of iterations.

$$\vec{D} = \left| \vec{C} \cdot \vec{X}^*(t) - \vec{X}(t) \right|, \quad (1)$$

$$\vec{X}(t+1) = \vec{X}^*(t) - \vec{A} \cdot \vec{D}, \quad (2)$$

where t shows the current iteration, \vec{A} and \vec{C} are coefficient vectors, \vec{X} is the position vector of the best arrangement acquired in this way, \vec{X}^* is the position vector, \cdot is the element by element multiplication and $|\cdot|$ is the absolute value. It merits saying here that \vec{X}^* should be upgraded in every cycle if there is a superior solution.

$$\vec{A} = 2\vec{a} \cdot \vec{r} - \vec{a}, \quad (3)$$

$$\vec{C} = 2 \cdot \vec{r}, \quad (4)$$

where \vec{a} is linearly decreased from 2 to 0 over the course of iterations and \vec{r} is a random vector in $[0, 1]$.

2.2. Bubble-net attacking technique

Here two methodologies are planned as follows:

1. **Shrinking encircling mechanism:** This behaviour is accomplished by diminishing the estimation of \vec{a} in Eq. (3). Take note of that the fluctuation range of \vec{A} is likewise diminished by \vec{a} . As such, \vec{A} will be a random value in the interim $[-a, a]$ where a is diminished from 2 to 0 throughout cycles. Random values for a vector \vec{A} are set in the range between $[-1, 1]$.

2. **Spiral updating arrangement:** Spiral condition for position update between humpback whale and prey that was helix-formed development given as takes after

$$\vec{X}(t+1) = \vec{D}' \cdot e^{bl} \cdot \cos(2\pi l) + \vec{X}^*(t), \quad (5)$$

where $\vec{D}' = |\vec{X}^*(t) - \vec{X}(t)|$ and shows the separation of the i th whale to the prey (best arrangement got as such), b is a steady to define the state of the logarithmic spiral; dot (\cdot) is a component by component augmentation and l is an arbitrary number in the range $[-1, 1]$.

To model so, we are assuming that there is a likelihood of picking a half between either the contracting surrounding system or the spiral model to overhaul the position of whales during enhancement. The scientific model is as per the follows:

$$\vec{X}(t+1) = \begin{cases} \vec{X}^*(t) - \vec{A} \cdot \vec{D}, & \text{if } P < 0.5, \\ \vec{D}' \cdot e^{bl} \cdot \cos(2\pi l) + \vec{X}^*(t), & \text{if } P \geq 0.5, \end{cases} \quad (6)$$

where P is an arbitrary number in the range $[0, 1]$.

2.3. Search for prey (exploration phase)

The \vec{A} vector can be utilized for exploration to search for prey; vector \vec{A} additionally takes the qualities more noteworthy than one or not as much as -1 . Exploration takes after the following two conditions:

$$\vec{D} = \vec{C} \cdot \vec{X}_{\text{rand}} - \vec{X}, \quad (7)$$

$$\vec{X}(t+1) = \vec{X}_{\text{rand}} - \vec{A} \cdot \vec{D}, \quad (8)$$

where \vec{X}_{rand} is an arbitrary position vector (an irregular whale) looked over the present population and calculated as when $|\vec{A}| > 1$, authorized investigation to WOA calculation to find worldwide ideal avoids local optima and when $|\vec{A}| < 1$, for overhauling the position of current search operator/best arrangement is chosen.

3. Modified whale optimization algorithm

In original WOA algorithm, the present best solution is the target for other search agents. Hence all prey attempt to modify their positions to proximate the best agent as per Equations (1) and (2). As the location of the best search, space is not known a priori, this process of update may result in being trapped in local optima. If the position of the vectors changes during the search, the process is governed by large steps, the algorithm may not be able to explore properly the search space. To minimize the magnitude of changes in the position of vectors, correction factors are introduced as CF_1 and CF_2 in the proposed mWOA technique. Now the equation becomes

$$\vec{D} = \left| \vec{C} \cdot \vec{X}^*(t) - \vec{X}(t) \right| / CF_1, \quad (9)$$

$$\vec{X}(t+1) = (\vec{X}^*(t) - \vec{A} \cdot \vec{D}) / CF_1. \quad (10)$$

The correction factor makes the whales to move in small steps towards the prey to explore the search space efficiently.

Similarly, a correction factor is introduced in the exploitation phase where the spiral updating position is given by Equation (11) as

$$\vec{X}(t+1) = (\vec{D}' \cdot e^{bl} \cdot \cos(2\pi l) + \vec{X}^*(t)) / CF_2. \quad (11)$$

By introducing the above correction factor, the humpback whales are made to swim around the prey within a

reduced shrinking circle, thus enhancing the exploiting capability of the algorithm.

Finally, the correction factor is introduced in the exploration phase of search for prey. So in original WOA algorithm, the search agent position is updated in the exploration phase as per Equations (7) and (8). As a result, it may lead to random movement of whales. Thus in the proposed mWOA technique, the position of search agents is updated by using correction factors as given in Equations (12) and (13).

$$\vec{D} = (\vec{C} \cdot \vec{X}_{\text{rand}} - \vec{X}) / CF_1, \quad (12)$$

$$\vec{X}(t+1) = (\vec{X}_{\text{rand}} - \vec{A} \cdot \vec{D}) / CF_2. \quad (13)$$

After a repeated series of trial runs, the correction factors are 2.5 and 1.5, respectively.

It should be noted that by introducing the correction factors, the capability of whales to reach any position in the search space is enhanced. Therefore, it allows any search agent to update its position in the neighbourhood of the current best solution and simulates encircling the prey more efficiently.

4. Performance investigation of mWOA algorithm

The proposed mWOA algorithm performance is carried out by fitting to some standard benchmark functions. The details about these functions, their dimension, boundary of the search spaces and optimum values are available in the literature [22]. There are 13 functions, out of which functions f_1 to f_7 are unimodal functions. Unimodal functions are specifically taken for verifying the exploitation property of the algorithm [22]. Functions f_8 to f_{13} are multimodal functions with more number of local optima. This number increases exponentially with the increase in dimensions. These functions are very challenging test beds for meta-heuristic algorithms as exploration and exploitation are tested simultaneously by these functions. As suggested in the original WOA algorithm, the mWOA algorithm is executed for 30 independent runs with randomly generated population for each benchmark functions with a population size of 30 and an

Table 1. Statistical result of proposed modified WOA and comparison with other techniques [22] for unimodal benchmark test functions.

f	mWOA		WOA		PSO		GSA		DE		FEP	
	Avg.	Std. dev.	Avg.	Std. dev.	Avg.	Std. dev.	Avg.	Std. dev.	Avg.	Std. dev.	Avg.	Std. dev.
f_1	0	0	1.41E-30	4.91E-30	0.000136	0.000202	2.53E-16	9.67E-17	8.2E-14	5.9E-14	0.00057	0.00013
f_2	0	0	1.06E-21	2.39E-21	0.042144	0.045421	0.055655	0.194074	1.5E-09	9.9E-10	0.0081	0.00077
f_3	0	0	5.39E-07	2.93E-06	70.12562	22.11924	896.5347	318.9559	6.8E-11	7.4E-11	0.016	0.014
f_4	0	0	0.072581	0.39747	1.086481	0.317039	7.35487	1.741452	0	0	0.3	0.5
f_5	28.7801	0.2426	27.86558	0.763626	96.71832	60.11559	67.54309	62.22534	0	0	5.06	5.87
f_6	5.4912	0.5014	3.116266	0.532429	0.000102	8.28E-05	2.5E-16	1.74E-16	0	0	0	0
f_7	0.1396E-4	0.144E-4	0.001425	0.001149	0.122854	0.044957	0.089441	0.04339	0.00463	0.0012	0.1415	0.3522

Table 2. Statistical result of proposed modified WOA and comparison with other techniques [22] for multimodal benchmark test functions.

f	mWOA		WOA		PSO		GSA		DE		FEP	
	Avg.	Std. dev.	Avg.	Std. dev.	Avg.	Std. dev.	Avg.	Std. dev.	Avg.	Std. dev.	Avg.	Std. dev.
f_8	-2.2973E3	0.4074E3	-5080.76	695.7968	-4841.29	1152.814	-2821.07	493.0375	-11080.1	574.7	-12554.5	52.6
f_9	0	0	0	0	46.70423	11.62938	25.96841	7.470068	69.2	38.8	0.046	0.012
f_{10}	4.086E-15	1.084E-15	7.4043	9.897572	0.276015	0.50901	0.062087	0.23628	9.7E-08	4.2E-08	0.018	0.0021
f_{11}	0	0	0.000289	0.001586	0.009215	0.007724	27.70154	5.040343	0	0	0.016	0.022
f_{12}	0.1815	0.1162	0.339676	0.214864	0.006917	0.026301	1.799617	0.95114	7.9E-15	8E-15	9.2E-06	3.6E-06
f_{13}	1.8095	0.1236	1.889015	0.266088	0.006675	0.008907	8.899084	7.126241	5.1E-14	4.8E-14	0.00016	0.000073

iteration of 500. Tables 1 and 2 show results like average and standard deviation for unimodal and multimodal functions, respectively. The proposed mWOA algorithm results were compared with the original WOA algorithm and with some recent well-known meta-heuristic techniques such as PSO, GSA, DE and FEP [22]. It is evident from Table 1 that, for unimodal modal functions, mWOA technique is very efficient and outperforms WOA, PSO, GSA, DE and FEP for five (f_1, f_2, f_3, f_4, f_7) out of seven unimodal test functions. It is observed from Table 2 that, mWOA outperforms WOA, PSO, GSA, DE and FEP for four (f_8, f_9, f_{10}, f_{11}) out of six unimodal test functions. This validates that the modified WOA makes a sound equilibrium between exploration and exploitation preventing local optima

stagnation. The proposed mWOA technique was then applied to a real-world problem of tuning the AFPID.

5. System investigated

The block diagram of the proposed system [1] is presented in Figure 1. The parameter of each component of system represents a real system and taken from reference [1]. The model under study was developed in MATLAB/SIMULINK environment and proposed mWOA program written (in .m file). The generation subsystem includes one PV, one DEG, one MTG, two FCs and three WTGs. The storage system includes one BESS and one FESS connected to the load side. Moreover, appropriate rate constraint nonlinearities

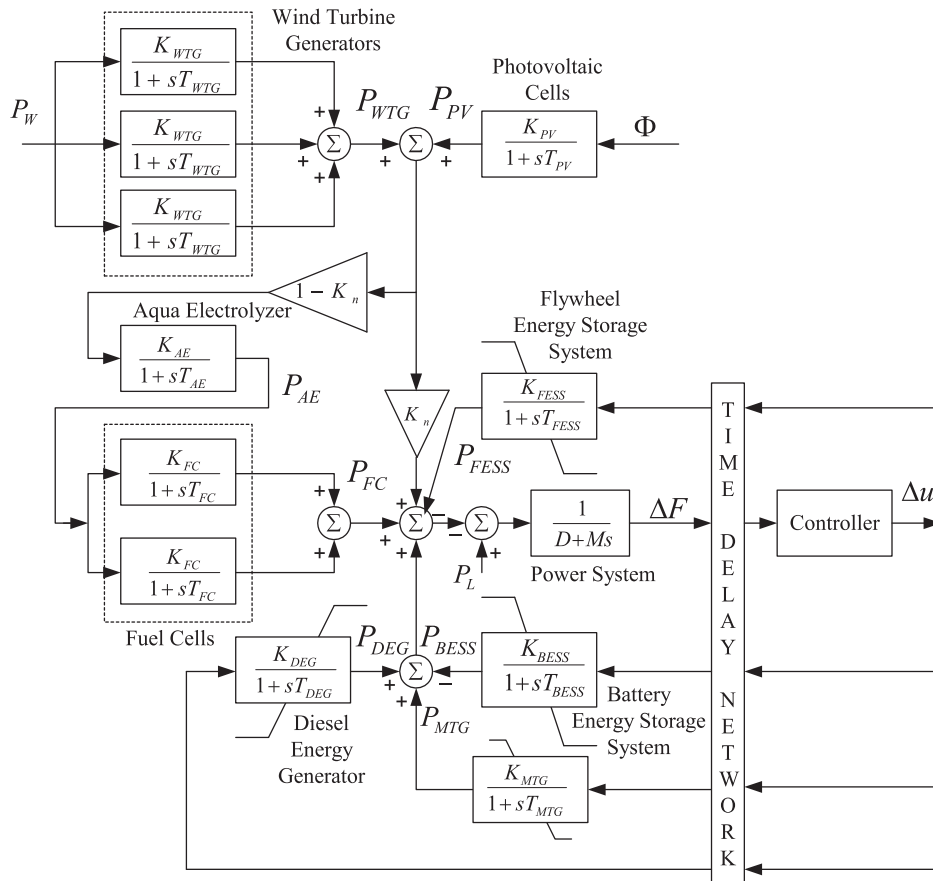
**Figure 1.** Block diagram representation of the APGS considered in the study.

Table 3. Parameters of APGS [1].

Components	Gain	Time constant
Solar photovoltaic (PV)	$K_{PV} = 1$	$T_{PV} = 1.8$
Wind turbine generator (WTG)	$K_{WTG} = 1$	$T_{WTG} = 1$
Aqua electrolyser (AE)	$K_{AE} = 0.002$	$T_{AE} = 0.5$
Fuel cell (FC)	$K_{FC} = 0.01$	$T_{FC} = 4$
Diesel energy generator (DEG)	$K_{DEG} = 0.003$	$T_{DEG} = 2$
Battery energy storage system (BESS)	$K_{BESS} = -0.003$	$T_{BESS} = 0.1$
Flywheel energy storage system (FESS)	$K_{FESS} = -0.01$	$T_{FESS} = 0.1$
Micro turbine generator (MTG)	$K_{MTG} = 0.002$	$T_{MTG} = 1$

were considered such as $|P_{FESS}| < 0.9$, $|P_{BESS}| < 0.2$, $|P_{DEG}| < 0.01$, $|P_{MTG}| < 0.01$. These rate constraint nonlinearities incorporate various electromechanical constraints that these devices exhibit.

5.1. Modelling of different generation system

The PV, DEG, MTG, FC and WTG are represented in Equations (14)–(18) with their corresponding gains and time constants reported in Table 3 [1,3,4]. The parameter k represents the number of units considered.

$$G_{PV}(s) = \frac{K_{PV}}{(1 + sT_{PV})} = \frac{\Delta P_{PV}}{\Delta \varphi}, \quad (14)$$

$$G_{DEG}(s) = \frac{K_{DEG}}{(1 + sT_{DEG})} = \frac{\Delta P_{DEG}}{\Delta u}, \quad (15)$$

$$G_{MTG}(s) = \frac{K_{MTG}}{(1 + sT_{MTG})} = \frac{\Delta P_{MTG}}{\Delta u}, \quad (16)$$

$$G_{FC_k}(s) = \frac{K_{FC}}{(1 + sT_{FC})} = \frac{\Delta P_{FC}}{\Delta P_{AE}}, k = 1, 2, \quad (17)$$

$$G_{WTG_k}(s) = \frac{K_{WTG}}{(1 + sT_{WTG})} = \frac{\Delta P_{WTG}}{\Delta P_W}, k = 1, 2, 3. \quad (18)$$

5.1.1. Wind speed modelling

The wind turbine generator power (P_{WTG}) is a function of wind speed V_W . The algebraic summation of base wind speed with noise component [1] is called as wind speed.

V_W can be represented by

$$V_W = V_{WB} + V_{WN}. \quad (19)$$

The base component of the wind speed is a constant which is present throughout the wind turbine operation and for the present case it is taken as 7.5 m/s. It is given as follows:

$$V_{WB} = 7.5\varphi(t) - 3\varphi(t - 200) + 10.5\varphi(t - 250), \quad (20)$$

where $\varphi(t)$ is the Heaviside step function.

The wind speed noise is given as follows:

$$V_{WN} = 2\sigma^2 \sum_{i=1}^N \sqrt{S_V(\omega_i) \Delta \omega} \cos(\omega_i t + \varphi_i), \quad (21)$$

where $\omega_i = (i - 1/2)\Delta\omega$ and $\varphi_i \approx U(0, 2\pi)$. $\Delta\omega$ is the change in frequency to estimate spectral density. σ^2 is the variance due to noise and set to 200.

The spectral density function $S_v(\omega_i)$ is expressed in (22)

$$S_v(\omega_i) = \frac{2K_N F^2 |\omega_i|}{\pi^2 \left[1 + \left(F \omega_i \frac{F \omega_i}{\mu \pi} \right)^2 \right]^{4/3}}, \quad (22)$$

where $N = 50$ and $\Delta\omega = 0.5$ rad/s are considered to get an operative modelling precision. K_N ($= 0.004$), μ ($= 7.5$) and F ($= 2000$) denote the surface drag coefficient, the base wind speed and the turbulence scale, respectively.

5.1.2. Wind turbine characteristic

The power coefficient of wind turbine (C_p) [1] is characterized by non-dimensional curves which is a function of blade pitch angle (β) and tip speed ratio (λ).

λ is given by

$$\lambda = \frac{R_{blade} \omega_{blade}}{V_w} \quad (23)$$

where R_{blade} ($= 23.5$ m) and ω_{blade} ($= 3.14$ rad/s) are the blade radius and blade rotational speed, respectively.

Considering $\beta = 0.1745$, C_p is given by

$$C_p = (0.44 - 0.0167\beta) \sin \left[\frac{\pi(\lambda - 3)}{15 - 0.3\beta} \right] - 0.0184(\lambda - 3)\beta. \quad (24)$$

The wind turbine output [1] is given by

$$P_w = \frac{1}{2} \rho A_r C_p V_w^3, \quad (25)$$

where $A_r = 1735$ m² is the blade swept area and $\rho = 1.250$ kg/m³ is the density of air.

5.1.3. Characteristic of PV system output power

The PV system output power of [1] is given by

$$P_{pv} = \eta S \gamma [1 - 0.005(T + 25)], \quad (26)$$

where η is the efficiency of the PV cells ($\eta = 10\%$), S is the area of the PV array ($S = 4084$ m²), γ is the solar radiation on the PV cells in kw/m² and T is the ambient temperature ($T = 25^\circ\text{C}$).

ϕ is given by

$$\phi = 0.5\varphi(t) - 0.33\varphi(t - 25) + 0.3\varphi(t - 75) - 0.3\varphi(t - 150) + \varphi_n(t),$$

$$\varphi_n(t) \approx U(-0.1, 0.1). \quad (27)$$

5.2. Modelling of aqua electrolyser

A portion of output power developed by wind and photovoltaic is used by an aqua electrolyser (AE). It produces hydrogen which is used by FC to produce power. AE uses a fraction, i.e. $(1 - k_n)$ of the total power generated from PV and WTG for the production of hydrogen which is fed to the two FCs to produce power. The transfer function of the AE can be sighted as

$$G_{AE}(s) = \frac{K_{AE}}{(1 + sT_{AE})}. \quad (28)$$

k_n is taken as 0.6 for the present study.

5.3. Modelling of energy-storing system

Energy-storing components effectively absorb/supply deficit/surplus energy from/to the hybrid power system within a fraction of period for a stable hybrid system [1,4].

FESS and BESS are two storage systems considered in the present study and are expressed as

$$G_{FESS}(s) = \frac{K_{FESS}}{(1 + sT_{FESS})} \quad (29)$$

$$G_{BESS}(s) = \frac{K_{BESS}}{(1 + sT_{BESS})}. \quad (30)$$

Each energy storage element is provided with an upper and lower saturation limit along with rate constraint nonlinearity to prevent the mechanical shock due to sudden frequency variation [6]. Their rate constraint nonlinearities are $|P_{FESS}| < 0.9$, $|P_{BESS}| < 0.2$ and $0 < P_{DEG} < 0.45$.

5.4. Power system model

The power system model is formulated as

$$G_{sys}(s) = \frac{\Delta f}{\Delta P_e} = \frac{1}{Ms + D}, \quad (31)$$

where D and M are equivalent damping constant (0.4) and inertia constant (0.03) of the hybrid power system, respectively. It is taken as 0.4 and 0.03 respectively for the present study.

6. Adaptive fuzzy logic control

A fuzzy logic controller has a predefined set of control rules, which depends on the researcher's knowledge and experience [23]. The input/output linguistic variables of the membership functions (MFs) are also generally predetermined. The design of FLCs largely depends on the choice of input/output scaling factors (SFs) and selection of controller parameters. Tuning of SFs is of highest importance because of their universal effect on the control action.

For satisfactory control action, the membership functions should be a function of error (e) and change of error (Δe) and FLC maps input to output by a limited number of IF-THEN rules. Sometimes, this is not adequate to provide necessary control actions. In such cases, static values of SFs and single MFs are insufficient to achieve the desired control action. To overcome this, various online and offline methods are proposed to fine-tune the input/output SFs to change the definition of MFs.

Adaptive control has been a topic of research for various LFC schemes. Adaptive control technique is categorized into two types, the self-tuning regulators and the model reference control systems [24]. Adaptive controller makes the system under control less sensitive to its parameter uncertainties under various environmental and operating conditions. Adaptive fuzzy-based PID controller design has now been considered as a topic of research and several methods are adopted in [14] and [24]. In the proposed method, an adaptive PID kind FLC (AFPID) is used to get the process optimally controlled based on the e and Δe . Figure 2 represents the schematic diagram of the proposed AFPID controller.

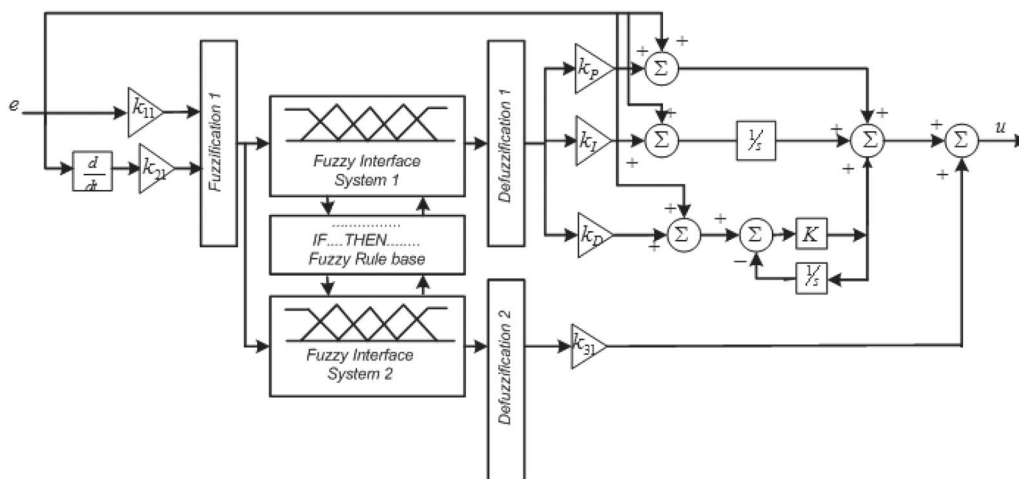


Figure 2. Structure of the proposed adaptive fuzzy logic control scheme.

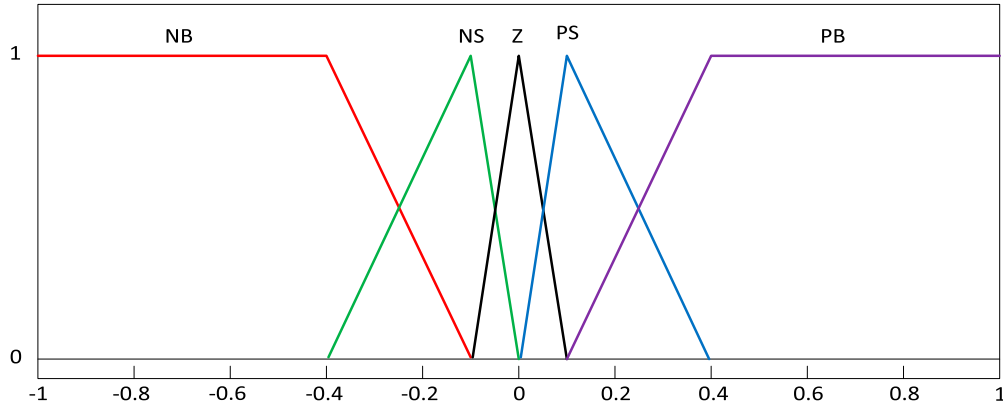


Figure 3. Membership function for e and \dot{e} .

Table 4. Rule base for AFPID.

e	\dot{e}				
	NB	NS	Z	PS	PB
NB	NB	NB	NS	NS	Z
NS	NB	NS	NS	Z	PS
Z	NS	NS	Z	PS	PS
PS	NS	Z	PS	PS	PB
PB	Z	PS	PS	PB	PB

Figure 3 shows the membership functions e and Δe and rule base is depicted in Table 4. Fuzzy part 1 and fuzzy part 2 share a common membership function. This makes the design simple. The MFs for e and Δe are kept within the common interval $[-1, 1]$ and they are chosen to be triangular which is the most popular and economical as compared to other alternatives. Mamdani fuzzy interface is used for the present simulation. The fuzzy linguistic variables NB, NS, Z, PS, PB represent Negative Big, Negative Small, Zero, Positive Small and Positive Big, respectively, and are shown in Table 6. The mWOA optimization algorithm is used for fine-tuning of the input and output scaling factors (k_{11} to k_{31}) and PID controller parameters (k_P , k_I and k_D) of AFPID controller shown in Figure 2.

ISE has taken into consideration in the present study for tuning of the controller gains

$$J = \int_0^{T_{\max}} [(\Delta f)^2 + (\Delta u)^2/K_f] dt, \quad (32)$$

where T_{\max} is the maximum simulation time and Δf and Δu are per unit frequency deviation and control signal output of controller. T_{\max} is taken as 300 s for the present case. The factor K_f is chosen as 10^4 to give equal weightage on both parts of control objective.

7. Results and discussion

7.1. Implementation of the proposed mWOA algorithm for frequency control

The APGS simulated by considering two different controllers, i.e. PID and AFPID controller separately and optimized with the mWOA technique. Figure 4(a–d)

depicts the stochastic output characteristics of the solar photovoltaic power (P_{PV}), wind turbine generator (P_{WTG}), renewable sources total power (wind and PV) to the electric grid (P_T) and the load demand (P_L) which is used in the simulation study. Both the solar and wind power output have overlying variations about their steady state, which would of course affect the system frequency. These oscillations have to damp out as quickly as possible by the proper control action of the controller. In the present design framework, both the powers (P_{WTG} and P_{PV}) drop to significantly different level after 25 and 200 s, respectively. This resembles the practical scenario as the generated powers of wind turbine and PV system fluctuate widely over time based on the varied environmental conditions. Simultaneously, the load demand also faces an identical kind of variation about its steady state and varies from 0.4 p.u to 0.9 p.u. The AFPID controller considers all these speculative variations while computing the controller gains. The optimized parameter of the PID and AFPID controller is given in Table 5. The corresponding values of objective function (J) are also given in Table 5. For the same controller structure (PID), minimum objective function value is obtained with the proposed mWOA technique ($J = 3.1809$) compared to the original WOA technique ($J = 3.5827$). The objective function value is further reduced ($J = 2.1809$) with the proposed mWOA optimized AFPID controller, i.e. there is a reduction of 39.13% in error criteria (objective function value) compared with the WOA optimized PID controller.

To compare the performance of designed controllers, various cases are assumed. For the first case, only the load variation as presented in Figure 4(d) is considered and wind and solar generations are kept constant. For the second case, solar generation, wind generation and load are variations that are considered as given in Figure 4.

Case 1: Load variation with constant wind and solar generation

In the first case, PV and wind powers are set constant (0.4 and 0.6 p.u., respectively), and the load demand is

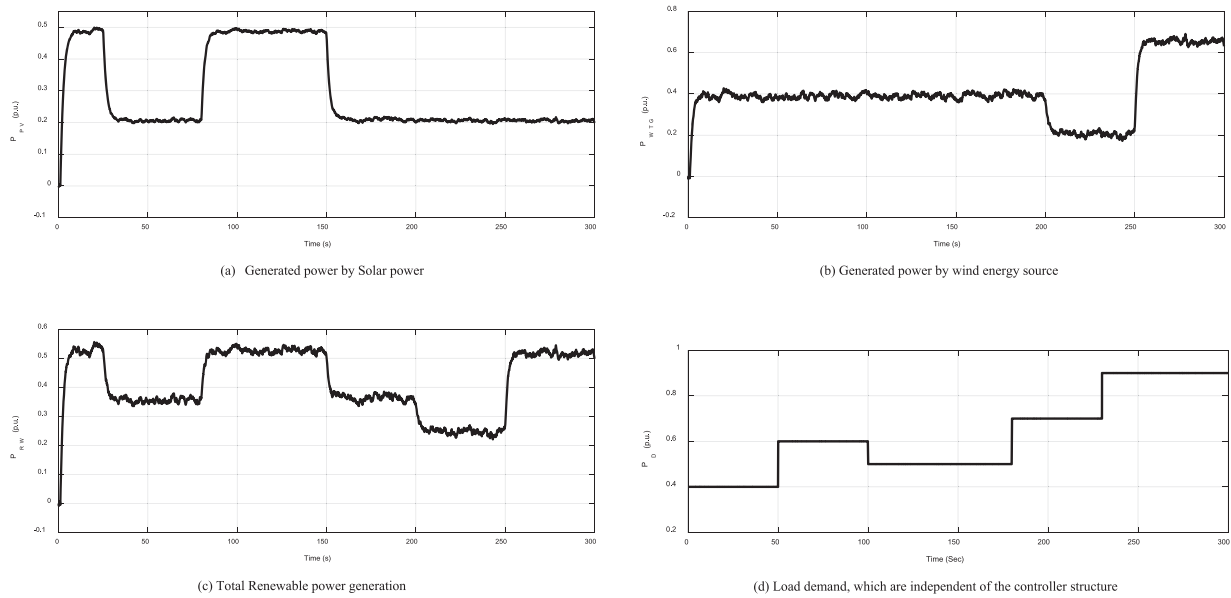


Figure 4. (a) Generated power by solar energy; (b) generated power by wind energy source; (c) total renewable power generation; (d) load demand which are independent of the controller structure.

Table 5. WOA- and mWOA-based tuning parameters of PID and AFPID controllers.

Technique/Controller	k_p	k_I	k_D	k_{11}	k_{21}	k_{31}	J
WOA: PID	8.8219	7.1508	4.4308	–	–	–	3.5827
mWOA: PID	9.2701	9.5176	1.8736	–	–	–	3.1809
mWOA: AFPID	4.8406	6.9087	0.2231	1.5893	1.6064	0.9664	2.1809

varied as shown in Figure 4(d). The frequency deviation for the above case is shown in Figure 5 from which it is clear that the mWOA optimized PID controller provides better system compared to the WOA optimized PID controller. It can be seen from Figure 5 that the maximum overshoot and undershoot with the WOA optimized PID controller are 0.3221 and -0.3599 and the same with the mWOA optimized PID controller are 0.3079 and -0.3645 , respectively. It is also clear from Figure 5 that the best system response is obtained with the proposed mWOA optimized FAPID controller. The maximum overshoot and undershoot reduce to 0.2697 and -0.1878 respectively with the mWOA optimized FAPID controller.

Case 2: Simultaneous variation of load demand, wind and solar power

In case 2, PV and wind powers varied as shown in Figure 4(a,b) along with the load variation. The system frequency response and control signal response are shown in Figure 6(a,b) respectively. For comparison, the responses with WOA optimized PID, mWOA optimized PID and mWOA optimized AFPID controllers are provided in Figure 6. From Figure 6(a) it is clear that the proposed mWOA optimized AFPID controller structure provides better system dynamic response compared to the WOA and mWOA optimized conventional PID control structure. It can be seen from Figure 6(a) that maximum overshoots with WOA

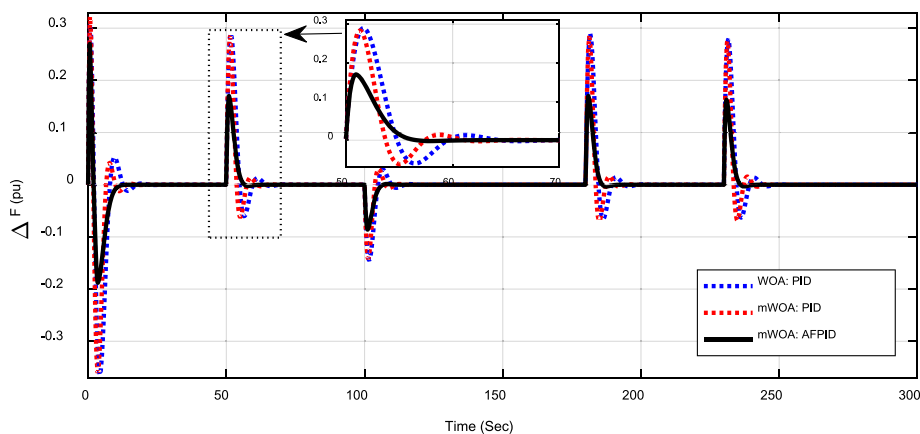


Figure 5. Frequency deviation response under load variation with constant wind and solar power.

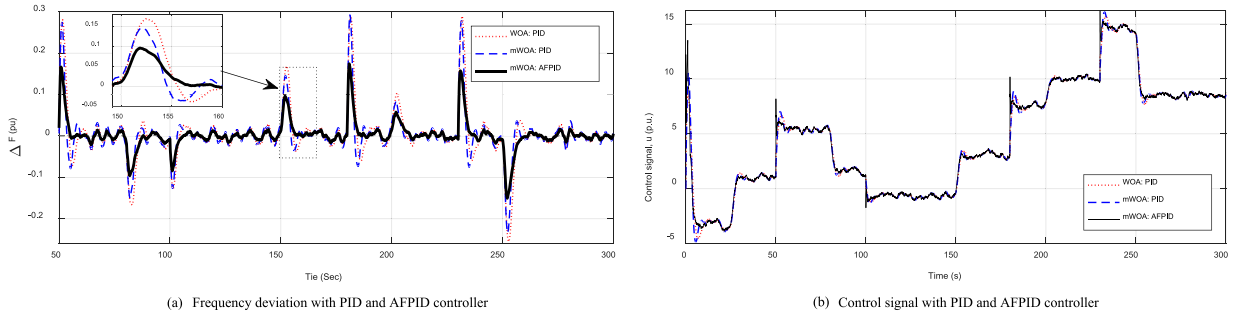


Figure 6. (a) Frequency deviation with PID and AFPID controllers and (b) control signal with PID and AFPID controllers.

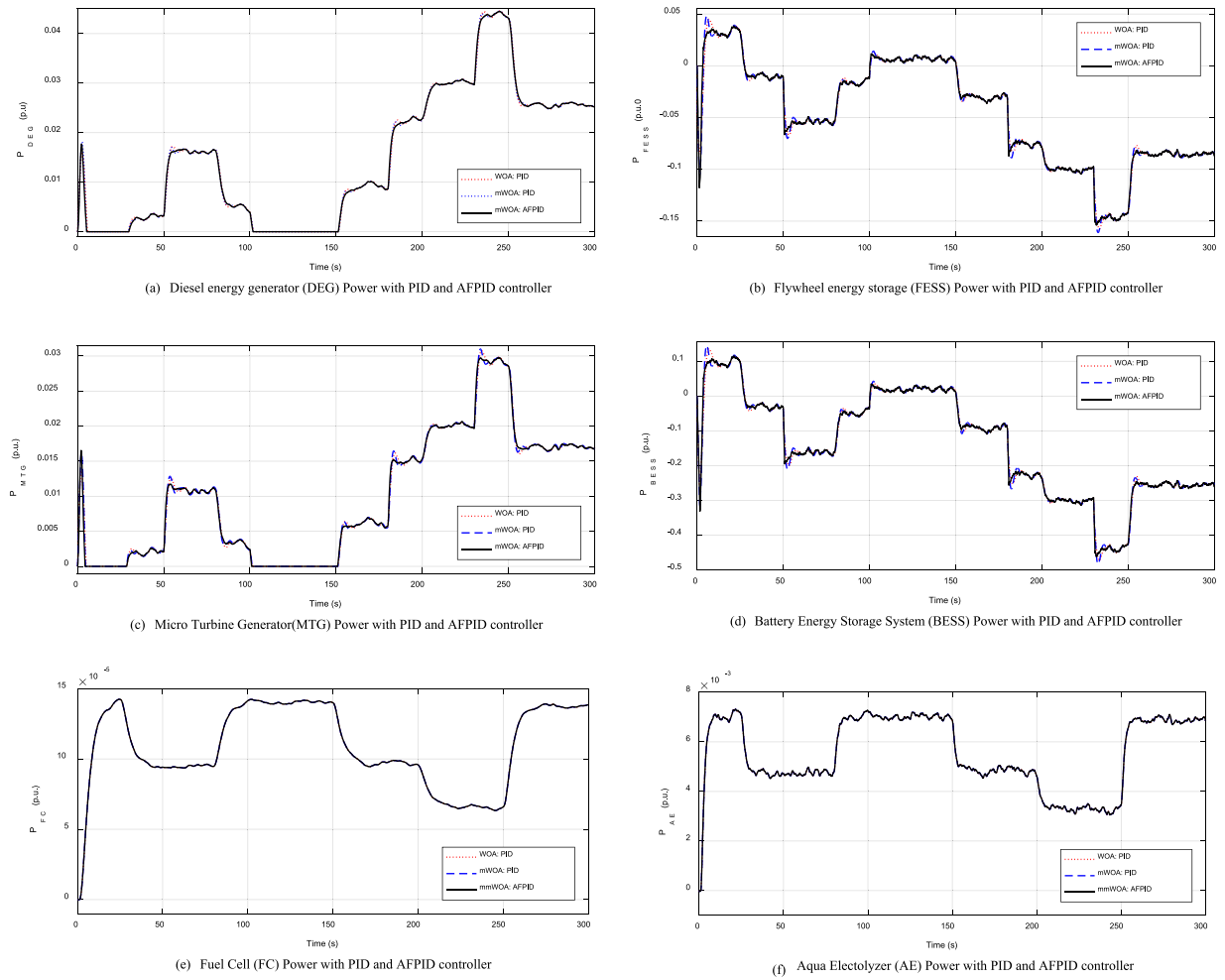


Figure 7. (a) DEG power with PID and AFPID controllers; (b) FESS power with PID and AFPID controllers; (c) MTG power with PID and AFPID controllers; (d) BESS power with PID and AFPID controllers; (e) FC power with PID and AFPID controllers; (f) AE power with PID and AFPID controllers.

optimized PID, mWOA optimized PID and mWOA optimized AFPID controllers during the first swing are 0.2806, 0.275 and 0.1666, respectively. Maximum undershoots are -0.2552 , -0.2339 and -0.1505 with optimized PID, mWOA optimized PID and mWOA optimized AFPID controllers, respectively.

From the control characteristic as shown in Figure 6(b), the band of oscillations for the AFPID controller is not as much as that of the classical PID controller. From practical point of view, this is relevant

as the control signal activates mechanical components such as DEG, BESS and FESS. Prolonged swinging in the actuator demand would deteriorate the mechanical parts, which degrade their lifetime as well as affect the performance of these components. The equivalent powers generated by the DEG, FESS, MTG, BESS, FC and AE are given in Figure 7(a–f). With the AFPID controller, the power fluctuation in these energy storage systems reduces significantly than that of the conventional PID controller. This may result in smaller

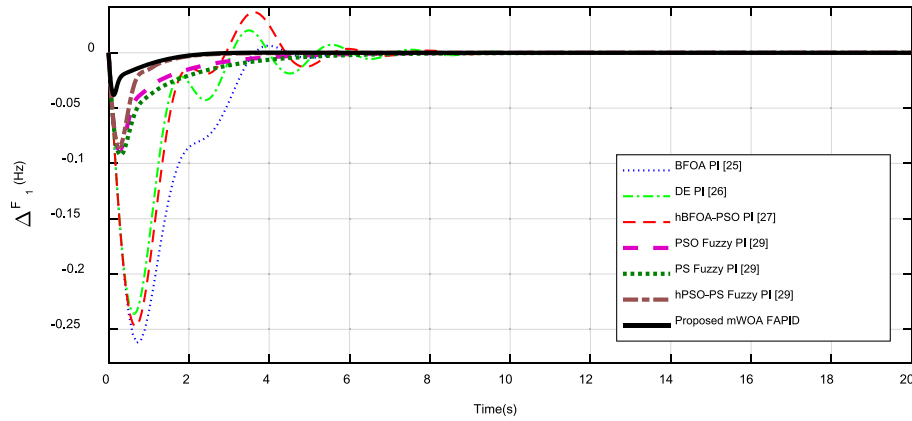


Figure 8. Frequency deviation of area 1 under step load disturbance in area 1 for a two-area non-reheat test system with different AGC approaches.

Table 6. Comparative performance indexes with recent AGC approaches.

Performance/technique: control structure	ITAE	value ($\times 10^{-2}$)	Settling times T_s (s)		Maximum overshoot	Maximum undershoot
			ΔF_1	ΔF_2		
Conventional ZN: PI [25]		375.68	45	45	18.25×10^{-2}	31.32×10^{-3}
GA: PI [25]		274.75	10.59	11.39	0	24.07×10^{-2}
BFOA: PI [25]		179.75	5.52	7.09	63.12×10^{-4}	26.21×10^{-2}
DE: PI [26]		125.51	8.96	8.16	20.26×10^{-3}	23.6×10^{-2}
PSO: PI [27]		121.42	7.37	7.82	38.58×10^{-3}	25.35×10^{-2}
hBFOA-PSO: PI [27]		118.65	7.39	7.65	36.73×10^{-3}	24.72×10^{-2}
NSGA-II: PI [28]		117.85	6.49	7.54	67.34×10^{-4}	26.32×10^{-2}
PS: Fuzzy PI [29]		63.34	6.05	7.10	0	92.08×10^{-3}
PSO: Fuzzy PI [29]		44.70	5.13	6.22	0	88.01×10^{-3}
NSGA-II: PIDF [28]		38.7	3.03	4.86	0	105.18×10^{-3}
hPSO-PS: Fuzzy PI [29]		14.38	2.26	3.74	0	85.18×10^{-3}
Proposed mWOA: AFPID		7.33	2.19	2.13	0	38.08×10^{-3}

dimension of this energy storage and supply systems. There is also less requirement of storing and supplying power to suppress the grid frequency variation. In Figure 7, negative powers in energy storage elements indicated that they are absorbing power and conversely the positive powers signify that they are producing the extra power making the whole system stable. Thus the hybrid power system becomes more reliable and energy efficient.

7.2. Comparison with recent frequency control approaches

To demonstrate the superiority of the proposed mWOA optimized AFPID controller, a widely used two equal area non-reheat thermal power system [25–29] is considered. Identical AFPID controllers are assumed for each area and the proposed mWOA algorithm was employed to tune the controller parameters. For a fair comparison, identical power system and objective functions from the literature [25–29] are considered. The optimized AFPID controller parameters are:

$$k_p = 1.9698, k_I = 1.7634, k_D = 1.0609,$$

$$k_{11} = 0.8172, k_{21} = 0.0777, k_{31} = 1.8405.$$

A step increase in demand of 10% applied at $t = 0$ s; in area 1 and the performance of proposed controller

is compared with approaches such as ZN: PI, GA: PI, BFOA: PI [25], DE: PI [26], hybrid BFOA-PSO: PI [27], NSGA-II: PI [28], NSGA-II: PIDF [28], PS: Fuzzy PI [29], PSO: Fuzzy PI [29] and hybrid PSO-PS: Fuzzy PI [29]. The results are provided in Table 6. It is clear from Table 6 that best system performance with minimum ITAE value and settling times in ΔF_1 , ΔF_2 and ΔP_{tie} are obtained with the proposed mWOA tuned AFPID controller compared to recently proposed AGC approaches. For completeness, the frequency response of area 1 for the above disturbance is shown in Figure 8. It is evident from Figure 8 that the proposed approach outperforms than recently proposed AGC approaches. The maximum overshoots and undershoots of frequency response are shown in Figure 8 and tabulated in Table 6. From Table 6, the lowest maximum overshoots and undershoots of frequency response are obtained with the proposed mWOA optimized AFPID compared to other approaches.

8. Conclusion

In practice, classical PID controller is commonly used for LFC problem. However, it is not able to provide desirable performance during severe disturbances. Owing to the practical difficulties faced in trying to achieve desired control criteria in LFC, an adaptive fuzzy logic PID control method is presented in this

paper for hybrid power systems. For tuning the controller parameters, a modified WOA technique is proposed where the position of search agents is updated by using correction factors. It is found from the statistical results that the proposed mWOA algorithm outperforms original WOA, PSO, GSA, DE and FEP algorithms. In the next stage, frequency control of an APGS consisting of various energy sources such as DEG, FC, MTG with renewable energy sources such as PV units, WTG along with energy storage devices like BESS and FESS and cluster of loads is considered and the parameters of proposed AFPID controller are optimized employing the mWOA technique. It is observed that the mWOA tuned AFPID controller provides superior performance compared to the PID controller. Testing the results of mWOA in terms of statistical analysis like “Wilcoxon Signed Rank Test” is the focus of the future work. Also, frequency control in an APGSs in the presence of plug in electric vehicles is the focus of the future research work.

Disclosure statement

No potential conflict of interest was reported by the authors.

ORCID

Subramani Chinnamuthu  <http://orcid.org/0000-0002-3745-2348>

Subhransu Sekhar Dash  <http://orcid.org/0000-0003-0861-8035>

References

- [1] Pan I, Das S. Fractional order AGC for distributed energy resources using robust optimization. *IEEE Trans Smart Grid*. 2016;7(5):2175–2186.
- [2] Ray P, Mohanty S, Kishor N. Small-signal analysis of autonomous hybrid distributed generation systems in presence of ultracapacitor and tie-line operation. *J Electr Eng*. 2010;61(4):205–214.
- [3] Lee DJ, Wang L. Small-signal stability analysis of an autonomous hybrid renewable energy power generation/energy storage system part I: time-domain simulations. *IEEE Trans Energy Convers*. 2008;23(1):311–320.
- [4] Ray PK, Mohanty SR, Kishor N. Proportional–integral controller based small-signal analysis of hybrid distributed generation systems. *Energ Convers Manage*. 2011;52(4):1943–1954.
- [5] Pan I, Das S. Fractional order fuzzy control of hybrid power system with renewable generation using chaotic PSO. *ISA Trans*. 2016;62:19–29.
- [6] Pan I, Das S. Kriging based surrogate modeling for fractional order control of microgrids. *IEEE Trans Smart Grid*. 2015;6(1):36–44.
- [7] Nandar CSA. Robust PI control of smart controllable load for frequency stabilization of microgrid power system. *Renew Energy*. 2013;56:16–23.
- [8] Singh VP, Mohanty SR, Kishor N, Ray P.K. Robust H-infinity load frequency control in hybrid distributed generation system. *Int J Electr Power Energy Syst*. 2013;46:294–305.
- [9] Mohanty SR, Kishor N, Ray PK. Robust H-infinity loop shaping controller based on hybrid PSO and harmonic search for frequency regulation in hybrid distributed generation system. *Int J Electr Power Energy Syst*. 2014;60:302–316.
- [10] Bevrani H, Feizi MR, Ataei S. Robust frequency control in an islanded microgrid H_{∞} and μ -synthesis approaches. *IEEE Trans Smart Grid*. 2015;7(2):706–717.
- [11] Pandey SK, Mohanty SR, Kishor N, Catalão J. P.S. Frequency regulation in hybrid power systems using particle swarm optimization and linear matrix inequalities based robust controller design. *Int J Electr Power Energy Syst*. 2014;63:887–900.
- [12] Senjyu T, Nakaji T, Uezato K, Funabashi T. A hybrid power system with using alternative energy facilities in isolated island. *IEEE Trans Energy Convers*. 2005;20(2):406–414.
- [13] Bevrani H, Habibi F, Babahajyani P, Watanabe M, Mitani Y. Intelligent frequency control in an AC microgrid: online PSO-based fuzzy tuning approach. *IEEE Trans Smart Grid*. 2012;3(4):1935–1944.
- [14] Savran A, Kahraman G. A fuzzy model based adaptive PID controller design for nonlinear and uncertain processes. *ISA Trans*. 2014;53(2):280–288.
- [15] Li X, Song YJ, Han SB. Frequency control in microgrid power system combined with electrolyzer system and fuzzy PI controller. *J Power Sources*. 2008;180(1):468–475.
- [16] Surender Reddy S, Bijwe PR, Abyankar AR. Fast evolutionary algorithm based optimal power flow using incremental variables. *Int J Electr Power Energy Syst*. 2014;54:198–210.
- [17] Surender Reddy S, Srinivasa Rathnam Ch. Optimal power flow using glowworm swarm optimization. *Int J Electr Power Energy Syst*. 2016;80:128–139.
- [18] Surender Reddy S, Bijwe PR. Multi-objective optimal power flow using efficient evolutionary algorithm. *Int J Emerg Electr Power Syst*. 2017;18(2):1–21.
- [19] Surender Reddy S, Praveen P, Kumari S. Micro genetic algorithm based optimal power dispatch in multi-mode electricity market. *Int J Recent Trends Eng*. 2009;2(5):298–302.
- [20] Surender Reddy S. Optimal power flow using hybrid differential evolution and harmony search algorithm. *Int J Mach Learn Cybern*. 2018: 1–15. doi:10.1007/s13042-018-0786-9
- [21] Surender Reddy S, Panigrahi BK. Optimal power flow using clustered adaptive teaching learning-based optimisation. *Int J Bio-Inspired Comput*. 2017;9(4):226–234.
- [22] Seyedali M, Lewis A. The whale optimization algorithm. *Adv Eng Softw*. 2016;95:51–67.
- [23] Fereidouni A, Masoum MA, Moghbel M. A new adaptive configuration of PID type fuzzy logic controller. *ISA Trans*. 2015;56:222–240.
- [24] Woo ZW, Chung HY, Lin JJ. A PID type fuzzy controller with self-tuning scaling factors. *Fuzzy Sets Syst*. 2000;115(2):321–326.
- [25] Ali ES, Abd-Elazim SM. Bacteria foraging optimization algorithm based load frequency controller for interconnected power system. *Int J Electr Power Energy Syst*. 2011;33:633–638.
- [26] Rout UK, Sahu RK, Panda S. Design and analysis of differential evolution algorithm based automatic generation control for interconnected power system. *Ain Shams Eng J*. 2013;4(3):409–421.

- [27] Panda S, Mohanty B, Hota PK. Hybrid BFOA-PSO algorithm for automatic generation control of linear and nonlinear interconnected power systems. *Appl Soft Comput.* **2013**;13(12):4718–4730.
- [28] Panda S, Yegireddy NK. Automatic generation control of multi-area power system using multi-objective non-dominated sorting genetic algorithm-II. *Int. J Electr Power Energy Syst.* **2013**;53:54–63.
- [29] Sahu RK, Panda S, Sekher GTC. A novel hybrid PSO-PS optimized fuzzy PI controller for AGC in multi-area interconnected power system. *Int J Elec Power Energy Syst.* **2015**;64:880–893.